Single Board Computing System for Automated Colorimetric Analysis on Low-Cost Analytical Devices

Journal:	*Analytical Methods*
Manuscript ID	AY-ART-08-2018-001874.R1
Article Type:	Paper
Date Submitted by the Author:	09-Oct-2018
Complete List of Authors:	Boehle, Katherine; Colorado State University, Chemistry Doan, Erin; Colorado State University, Computer Science Henry, Sadie; Colorado State University, Computer Science Beveridge, Ross; Colorado State University, Computer Science Pallickara, Sangmi; Colorado State University, Computer Science Henry, Charles; Colorado State University, Chemistry;

Single Board Computing System for Automated Colorimetric Analysis on Low-Cost Analytical Devices

Katherine E. Boehle[1], Erin Doan[2], Sadie Henry[2], J. Ross Beveridge[2], Sangmi L. Pallickara[2], Charles S. Henry[1,3*]

Departments of Chemistry[1], Computer Science[2], and Biomedical Engineering[3], Colorado State University, Fort Collins, Colorado

Abstract

Colorimetric detection, while a user-friendly and easily implemented method of analysis on low-cost analytical devices, often suffers from subjectivity by the device user. We describe the development of a single board computing system to automatically analyze colorimetric samples. Single board computing systems such as Raspberry Pi, offer significant computing power in a small, inexpensive package. By programming an attached camera to obtain images every minute, we demonstrated that Michaelis-Menten enzyme kinetic constants can be calculated directly from paper and transparency devices based on the change in color intensity over time in seconds instead of hours using an integrated image analysis program. In this system, a 3D-printed box was designed and optimized with an independent lighting system that holds the paper-based devices and the Raspberry Pi board and camera. The box omits environmental and ambient light for consistent lighting and holds the camera at a constant focal length. While early versions of the image analysis program used single pixels, the final program uses a flood fill algorithm for colorimetric analysis so the system is not restricted by device shape and can discriminate discoloration due to lighting, making it adaptable to other colorimetric device applications. As a proof-of-principle, we compared enzyme kinetics between Whatman chromatography paper and transparency-based devices and found that changing the platform did not compromise the apparent V_{max} and K_M calculated by the program.

1
2
3
4
5
6
7
8
9
10
11
12
13
14
15
16
17
18
19
20
21
22
23
24
25
26
27
28
29
30
31
32
33
34
35
36
37
38
39
40
41
42
43
44
45
46
47
48
49
50
51
52
53
54
55
56
57
58
59
60

Introduction

The need to take advanced laboratory tests into resource-limited settings has sparked the field of portable lab-on-a-chip sensors. These devices have enabled users to measure specific analytes in the field without transporting samples to a central laboratory for expensive testing.[1-3] The desire for simple, inexpensive devices has driven the field of microfluidic paper-based analytical devices (μPADs), which have grown significantly in popularity since 2007.[4-6] Paper-based devices have been developed for portable detection of environmental contaminants,[7, 8] foodborne pathogens,[9, 10] infectious diseases,[11-13] and other health ailments.[14, 15]

Paper-based devices allow for many different detection motifs including colorimetry, electrochemistry, fluorescence, or chemiluminescent detection.[4, 16, 17] Colorimetric detection provides one of the simplest options for in-field analysis as it does not require external instrumentation. However, color-intensity-based measurements can suffer from subjective reading, causing inconsistent results between tests and users.[17] To help combat this problem, colorimetric devices based on length of a colored band have been developed.[16, 18] Like an analog temperature thermometer, the user simply measures the length of color to determine analyte concentration. However, an advantage of color-intensity-based spot tests is the ability to capture kinetic information. Distance-based devices also tend to have lengthy analysis times (typically 30 min) and the devices are not as easily fabricated. Additionally, not all analytes, such as cellular organisms like bacteria and fungi, are able to efficiently move through paper due to limited pore sizes.[10]

Currently, most colorimetric devices using color intensity require images to be captured with a digital camera or desktop scanner and then the image analyzed using imaging software. While this setup works for laboratory settings, it is not as applicable to field settings for a variety of reasons. Whitesides and coworkers were the first to suggest the use of cellphones for offsite real-time diagnosis, where the healthcare provider captures an image using a cellphone

camera, then sends the image for offsite image analysis and official diagnosis.[19] With the rapid

growth and deployment of smartphones worldwide, it is no longer necessary for images to be

sent offsite for analysis. Smartphones are capable of storing and running complex applications

for chemical analysis, including image capture and automated analysis. Applications like these

have been developed for paper-based devices for water quality monitoring[20] and *Salmonella*

detection,[21] to name a few.[22] Although smartphones have opened the door for a variety of

possibilities for portable medicine and environmental monitoring when combined with paper-

based devices, there are drawbacks. The average cost of a smartphone is over \$300 worldwide,

a statistic that has not decreased since 2011.[23] Additionally, smartphones are frequently

updating software and imaging applications need to update with the software for compatibility.

Programmers developing applications for point-of-care diagnostics also need to consider the

Health Insurance Portability and Accountability Act, a United States legislation that was

introduced in 1996 to protect individual medical information. Constantly changing software can

breach protection when using wireless smartphones for sensitive medical information.[24]

Raspberry Pi's one example of inexpensive, portable single-board computers that have

become popular because they are easy to program for a variety of uses.[25] While commonly

used for automation of household appliances such as temperature, lights and home security,[26,

27] Raspberry Pi computers can also be programmed for automating scientific analysis.[28, 29]

Furthermore, specialized cameras have been developed for Raspberry Pi boards that can be

controlled through programming.[30] A Raspberry Pi system has been created for automatic color

analysis in colorimetric assays, but this system is for analyzing color in solution, not on paper-

based devices.[31] In addition to programming the Raspberry Pi to automatically analyze images

after capture,[32] these images can be captured at specific times points, enabling kinetic analysis.

One of the most common detection motifs used in μPADs are enzymatic reactions,

including the first μPAD, which was developed for glucose detection.[6] Enzymes are an attractive

detection motif because of their selectivity, specificity, and catalytic abilities to amplify a product,

yielding lower detection limits. Beyond glucose detection, enzymes have been used in the detection of urine creatine, cholesterol, and pesticides, to name a few.[15, 33-35] In addition to using enzymes to detect specific substrates, enzyme detection can be used for clinical diagnostics[36-38] and measuring pathogens.[39, 40] Because of the common employment of enzymes in paper-based devices, it is important to understand how paper affects an enzymatic reaction. Studies have demonstrated the impact of paper substrate on the formed color intensity, and how different papers affect nucleic acid amplification.[41, 42] To the best of our knowledge, however, there has not been a study completed that directly analyzes changes in enzyme kinetic parameters depending on the device substrate.

Herein, we describe the development of a single board computing system based on a Raspberry Pi unit for the automatic calculation of Michaelis-Menten enzyme kinetics on different portable device substrates. We have developed a 3D-printed light box that holds the Raspberry Pi computer board, attached camera, and devices. This light box allows for an independent light source, reducing variability of ambient lighting, and consistent placement of the camera and devices. A program was developed for precise and accurate analysis using a flood-fill algorithm to analyze the color intensity directly on the devices. Using this system, we have measured enzyme kinetics with paper or transparency film devices. While this analysis system was specifically programmed for obtaining and analyzing a series of colorimetric images, then automatically calculating Michaelis-Menten constants V_{max} and K_M, the program could be modified for other applications on paper-based devices and eliminate subjectivity in reading colorimetric devices.

Materials and Methods

Materials. A Raspberry Pi 2 Model B was used along with a Wide Angle FOV160° Raspberry Pi camera [SainSmart] attached to the computer board with a 15-pin ribbon cable. The camera contains a Omnivision 5647 sensor in a fixed focus module with 5-megapixel

resolution. The Raspberry Pi board was enclosed in a transparent case that allowed access to all ports while also protecting the internal components [SB Components]. The enzyme kinetic experiments were carried out with two enzyme/substrate pairs, β-lactamase [Abcam] and nitrocefin [VWR International] and β-glucuronidase [Sigma] and p-nitrophenol-β-d-glucuronide [Sigma].

Paper-Based Device Fabrication. Substrates used for testing were Whatman 1 chromatography paper [GE Healthcare Sciences] and clear plastic transparency film [Apollo]. A simple 9 by 8 grid design of 7 mm black circles was designed with CorelDRAW. To define hydrophobic barriers, a ColorQube 8870 [Xerox] wax printer was used to dispense wax on the paper or plastic's surface and an IsoTemp [Fisher Scientific] hot plate was set to 150 °C with two metal plates on it. Wax-printed paper was placed between the hot plate and a metal plate for 60 s for the wax to melt through the paper. This step was omitted for transparency film. After cooling, Scotch Shipping Heavy Duty packing tape was used to cover the back of the paper-based devices to prevent sample leakage. The paper-based devices were laser-cut to be 9.4 x 9.4 cm with four 3 mm holes located one each at each corner for the paper-based devices to fit onto the pegs designed into the device holder. The laser cutter used was an Epilog Zing Laser Cutter (30 Watt) set to 100% speed, 9% power, and 2500 Hz frequency.

Designing and Fabricating the Raspberry Pi Holders. The holder for both the Raspberry Pi computer board/camera and the paper-based devices were designed using computer-assisted design software and 3D printing. CAD files are publically available on our website (http://wp.natsci.colostate.edu/henrylab/). All components were 3D printed using clear resin and a Form 2: Stereolithography 3D Printer [Formlabs]. The bottom component of the holder, which holds the paper-based devices, was designed using SketchUp [Microsoft]. This device holder component measures 10.4 x 10.4 cm with a 3 mm lip that allows for the top component (that holds the Raspberry Pi card and camera) to consistently sit in a set position. 3 mm pegs in the floor of the holder were used to consistently align the paper and transparency

devices. The devices had 3 mm holes cut in the exact locations of the pegs located in the holder. The walls of the holder are 5 mm thick to compensate for the 3 mm lip, and the floor of the holder is 3 mm thick.

Raspberry Pi and Camera Holder Design. The final Raspberry Pi holder was designed using Onshape, a cloud-based CAD software. The holder measures 10 x 10 x 10 cm. Pegs were designed into one side of the holder to hold the Raspberry Pi board (housed in transparent case) and measured 4 mm at the base and 6 mm at the top. The case enclosing the Raspberry Pi board contains notches for wall mounting that the pegs were specifically designed to hold so the Raspberry Pi board case would snap into place. The lid of the holder also measures 10 x 10 cm and is 3 cm deep, making the entire holder 13 cm tall. The lid was attached to the body of the holder by attaching metal hinges to both the lid and the body using Epoxy glue. The walls of the holder, both the lid and body, were 3 mm thick. To hold the camera, the user lifts the lid and places the camera on pegs that were designed to fit into holes designed into the camera. The camera is placed in the center of the holder through a 15 mm diameter circle. The camera holder was held in the center of the device using 3 mm diameter supports leaving most of the device open for the light source to illuminate the devices. A light diffuser was created to sit on the camera holder supports. The light diffuser was made with clear poly(methyl methacrylate) (PMMA) and cut to be 9.4 x 9.4 cm with a 2.5 x 2.9 cm square cut out of the center for the Raspberry Pi camera to lay flat. To give the PMMA a frosted texture, sandpaper and water was used to lightly scratch the surface of one side of the polymer. The light circuit was designed to fit into the lid of the Raspberry Pi holder so the lighting was placed behind the Raspberry Pi camera. 16 LEDs were arranged in a circle by laser-cutting two 3 mm holes in white PMMA for each LED to be placed in a circle orientation. The wires from each LED were inserted into the 3 mm holes and were wired in parallel. All anodes and cathodes of each LED were soldered to a circular copper wire ring to eliminate the need for 32 separate wires. One wire was soldered to each the "anode ring" and the "cathode ring." A light circuit was generated by wiring a 9V battery

to a toggle switch, then to the light bulbs in parallel, then to a 100 Ω resistor, back to the negative input of the battery. Hot glue was dried over the wiring to insulate the electrical connections. The light circuit in the PMMA board was glued in the lid of the Raspberry Pi holder also using Epoxy.

Lighting System Considerations. A paper-based device without any samples was placed in the bottom of the device holder and several different lighting conditions were tested. This includes whether the light diffuser was necessary; if the frosted side of the diffuser should face towards or away from the devices; whether lining the side of the holder with copy paper would help diffuse light (with and without the first light diffuser); and covering the entire device with a dark cover to further limit exterior light. Images were captured using the Raspberry Pi camera and analyzed using ImageJ by measuring the light intensity of each sample spot after selecting the green color channel, without inverting the image. The ideal lighting system was selected by calculating the standard deviation from each row and column and averaging all standard deviations. The most consistent lighting was selected to give the smallest average standard deviation across all sample spots. A heat map was generated in Microsoft Excel for a visual demonstration of light distribution across the sample spots on the paper-based device. In the heat maps, green represents lower light intensity while white represented higher light intensity.

Kinetic Experiments and Analysis. For reactions between nitrocefin and β-lactamase, nitrocefin was diluted with pH 7.4 phosphate buffered saline (PBS) [1.37 M NaCl, 0.027 M of KCl, 0.1 M Na_2HPO_4, and 0.018 M KH_2PO_4] to the following concentrations for enzyme kinetic experiments: 0.05, 0.1, 0.25, 0.4, 0.5, 0.6, 0.7, and 0.9 mM were used to generate a kinetic curve. For reactions between β-glucuronidase and p-nitrophenol-β-d-glucuronide (PNP-glucr), the substrate and enzyme were also dissolved in pH 7.4 PBS. The same concentrations were used to obtain a kinetic curve for PNP-glucr as nitrocefin. 6 Unit mL^{-1} and 300 Unit mL^{-1} concentrations were used for β-lactamase and β-glucuronidase respectively. To generate a

calibration curve for nitrocefin, concentrations of 0.01, 0.025, 0.05, 0.075, 0.1, 0.15, 0.2, and 0.25 mM were used. For p-nitrophenol, concentrations of 0.05, 0.1, 0.2, 0.3, 0.4, 0.5, 0.6, and 0.7 mM were used.

For each experiment, three samples of each reaction were placed in every other column of circles. The columns on each side of the samples were used for water to act as a "light control." This concept is described in detail in previous publications.[9, 13] For manual analysis, the images were analyzed using NIH ImageJ software. The image was split into red, green, and blue color channels and the green (β-lactamase) or blue (β-glucuronidase) color channel was selected and inverted (Figure SI1). The intensity of each color spot was quantified using the circle tool, then normalized by subtracting the average brightness of the water spots on each side of the sample spot. After normalization, color intensity was converted to product concentration using a calibration curve. Instead of inputting a different calibration curve for each experiment, a calibration curve was implemented into the paper-based device in the eighth column. The calibration curve was generated by plotting color intensity *vs.* known product concentration (either hydrolyzed nitrocefin or p-nitrophenol as products) and generating a linear regression line. Color intensity was converted to product concentration by inputting color intensity into the "Y" variable, and calculating "X", the product concentration. While p-nitrophenol as a product is available commercially, hydrolyzed nitrocefin is not. A calibration curve for nitrocefin was obtained by reacting nitrocefin with 100 U mL^{-1} β-lactamase for 1 hr, and the assumption is made that 100% of nitrocefin is hydrolyzed.

To calculate Michaelis-Menten parameters, images were captured at minutes 1, 2, and 3, to represent reaction progression (Figure SI3). To calculate the reaction rate, the product formed (calculated using the linear regression equation as described) at each time point was calculated and plotted on a graph of product formed *vs.* reaction time. The slope of the linear regression was determined to be the reaction rate in units of mM min^{-1}. The rate of eight different concentrations of each substrate were used to obtain a kinetic curve. V_{max} and K_M

values were calculated for each enzyme and substrate pair by generating a Lineweaver-Burk plot. 1/[S] was plotted *vs.* 1/v and the inverse x- and y-intercepts were obtained. The calculated V_{max} and K_M values were carried out in the Michaelis-Menten equation to obtain a theoretical kinetic curve to compare to the data points and verify the accuracy of the calculated V_{max} and K_M.

Using the Raspberry Pi. The Raspberry Pi was programmed to obtain images every minute for three minutes and analyze the color intensity by selecting a specific pixel from each sample spot in the image. Then using a flood fill algorithm, the program analyzes the color intensity of the pixels surrounding the first pixel. If the surrounding pixels are within a selected threshold, the pixels are included in an overall average color intensity. Collecting and analyzing the surrounding pixels continues until the program reaches pixels not within the color intensity threshold, such as inconsistent lights or the edge of the device. The kinetic parameters are calculated as described above for manual analysis in obtaining V_{max} and K_M.

To perform data analysis on a Raspberry Pi in real-time, we have designed and developed a software, KineticsAnalyzer. Code files are publically available on our website (http://wp.natsci.colostate.edu/henrylab/).As depicted in Figure SI2, KineticsAnalyzer performs a series of data analysis and manages interactions with input devices and local storage units (e.g. local file system and database server). The system includes 5 core software components: Image Sensor Input Manager, Data Parser, Data Calibrator, Data Analyzer, and Analyzer Output Manager. These software components are extensible to assimilate new sensing input devices or output storage systems.

The Image Sensor Input Manager interacts with the camera and stores images. Once the pixel information is captured, the Data Parser scans data to select a relevant area within the image and extracts those pixels. The Data Parser organizes values based on the column and row numbers of the image pixels. Data Calibrator computes summary statistics of the values of

target pixels and normalizes it. The Data Calibrator also computes slopes and intercepts over

the preprocessed data points. Using the slope intercept calculated in Data Calibrator, Data

Analyzer finds concentrations of the target pixels. Finally, the Vmax and Km are computed using

combined values. The Analyzer Output Manager stores results in the local database system,

MySQL, through a JDBC connector. This allows remote users to search and retrieve results with

more expressive queries.

Results and Discussion

       Designing a Raspberry Pi and Device Holder. In addition to programming the

Raspberry Pi, one of the first steps was to design a holder to house the paper- and

transparency-based devices and hold the Raspberry Pi board with attached camera. This holder

was designed to make the system more portable and user-friendly, and for consistent

placement of the devices and holding the Raspberry Pi camera at a consistent focal length.

Additionally, one of the recognized pitfalls of using computer programs for analysis is variable

lighting conditions found in field settings.[43] Creating a holder with an independent lighting

system should eliminate this problem by controlling lighting. The final holder has two

components: the bottom component to hold the paper- and transparency-based devices for

consistent placement, and a top component to hold the Raspberry Pi, attached camera, and

lighting system. For a lighting system that best illuminated the devices, we designed the holder

for the light source to be placed behind the camera for the lights to not be in the camera's frame

of view. This was accomplished by making the holder square and adding a lid (Figure 1). A

circular ring containing 16 LEDs was glued into the lid (Figure 1B) allowing the lid to close over

the camera situated in the center of the holder (Figure 1C). Frosted PMMA was used as a light

diffuser, which is further discussed below. The bottom component of the holder was designed to

hold the devices in the same location between experiments. 3 mm pegs were designed in the

bottom component, and 3 mm holes were cut into the devices via laser cutting in the same location as the holder's pegs for consistent device placement (Figure 1D and 1E).

Optimizing Lighting in the Raspberry Pi Holder. To generate the best lighting system, we compared light distribution using one of several light diffusing methods. Light distribution was compared by measuring the light intensity of each sample spot on a clean paper-based device. The standard deviation of light intensity in each row and column of the paper-based device were calculated, then all standard deviations were averaged. The smaller the average standard deviation (SD), the more evenly distributed the light. For a visual comparison, heat maps were generated to visualize light distribution. In addition to testing whether the frosted plastic light diffuser was necessary, we also investigated the position of the frosted plastic diffuser in the holder, lining the inside of the holder with white copy paper, and putting a dark cloth over the entire holder to limit exterior light. The best distribution of light was accomplished with the frosted diffuser, with the frosted side facing the paper-based device, lining the holder with white copy paper, and without a dark cover over the holder. The average standard deviation of light intensity (arbitrary units) across the PAD was 4.85 (highlighted in Figure 2A), which was much lower than the average light intensity SD of 15.20 seen in the worst light distribution (no light diffusers) in Figure 2B.

The use of a dark cover over the holder consistently resulted in less light distribution across all experiments. This is surprising when considering a dark cover was necessary in the first iteration of a Raspberry Pi holder (more details of this first iteration in the Supporting Information). The difference is likely because the final holder encloses the camera in the holder, unlike the first iteration of the holder where the camera sat on top of the holder and imaged the PAD through a viewing window. By sitting on top of the holder, environmental light easily affects image capture. Because the holder is fabricated with clear resin, exterior light can still penetrate the inside the holder. Lining the interior of the holder with copy paper likely assisted with limiting

exterior light, plus these experiments were completed indoors with consistent environmental lighting. Therefore, this is an aspect that could change when the system is used outdoors.

The Raspberry Pi Program. When the program was first generated, the color intensity was quantified on devices by analyzing one pixel in each sample spot (for more information on the initial code, see Supporting Information). The analysis suffered, however, if the selected pixel was not representative of the entire sample zone, resulting in significant error. To overcome this limitation, the program was updated with a flood-fill algorithm. Similar to the first program, one pixel is selected, but then the program analyzes the color intensity of the pixels surrounding the first pixel. If the color intensity of each additional pixel is a similar color intensity range (within a selected threshold), then the new pixels are included in the overall average. Once included in the overall average, then the pixels around that pixel are analyzed. If a pixel is not within the color intensity threshold, the pixel is omitted. Therefore, once the program reaches the end of the sample area, it will stop including pixels in the overall average as the pixels in the wax barrier will not be in the color intensity threshold. This code should provide more accurate results compared to manual analysis for reasons by allowing for customizable sample zones, eliminating subjectivity, and avoiding zones within a spot that have inconsistent lighting. In manual analysis, a single oval shape is created to encompass the entire sample zone during using the circle tool in ImageJ. The same oval is used throughout analysis for consistency and analysis speed. However, using a wide-angle fisheye lens for the Raspberry Pi system causes inconsistently shaped spot images, which are visible when comparing Figure SI1 (obtained with a camera phone) and Figure SI3 (obtained with the Raspberry Pi camera). Using the flood-fill algorithm solves this problem.

Enzyme Kinetics Analysis *vs*. Manual Analysis. To verify the accuracy of the Raspberry Pi program analysis, we compared manual analysis to analysis by the Raspberry Pi program for obtaining Michaelis-Menten enzyme constants V_{max} and K_M. Two different enzyme/substrate pairs were used, β-lactamase with nitrocefin, a colorimetric reaction from

yellow to red, and β-glucuronidase with p-nitrophenol-β-d-glucuronide (PNP-glucr), a reaction

that turns from clear to yellow on paper-based devices. V_{max} values varied by 1% to 11%

between manual and automated analysis (Figure 3A), compared to 10% to 43% off when using

only one pixel for analysis. Values of K_M displayed larger error, 2% to 17% (Figure 3B),

however, this is still an improvement from analyzing one pixel, which could be off by up to 44%.

The accuracy of obtaining colorimetric values using the flood-fill algorithm was further

verified when obtaining V_{max} and K_M on transparency-based devices. Due to the reflectiveness

of plastic, error was introduced into the sample spots by the ring of lights despite the use of the

optimized light diffusers (Figure 4). Whatman filter paper is matte white, helping to distribute

light in addition to the diffusers. Despite placing copy paper under the transparency sheet,

plastic still reflects the light. In the transparency sheet kinetics images, one can see the

reflection of the light ring in the sample spots. In addition, the images exhibit minor spherical

aberration due to the working distance of the system. For both problems, when the specific color

channel is obtained and inverted, this light ring reflection turns into black spots, and can

therefore affect the color intensity when averaging the entire sample spot (Figure 4A). However,

the flood-fill algorithm can avoid these light spots because the pixel values are not within the

program's threshold. The light spots are eliminated from the overall average using the flood fill

algorithm (Figure 4B), which would not be possible using manual analysis.

Kinetics on Different Device Substrates. When comparing enzyme kinetics between

paper and transparency devices, we used the values obtained by the updated Raspberry Pi

program. Because of the program's ability to avoid reflections from the light source seen in

transparency-based devices, the program likely obtains more accurate results compared to

manual analysis. Preliminary results show kinetic values for β-lactamase and β-glucuronidase

on Whatman paper are comparable to kinetics on transparency film (Figure 5A). This indicates

that despite changing the reaction platform from plastic to paper, the apparent enzyme kinetics

are not compromised. When Linnes et al determined the effects of different paper substrates on

isothermal nucleic acid amplification, it was concluded that using chromatography or filter paper nearly completely inhibited amplification.[44] It was hypothesized that enzymes associated with amplification were nonspecifically adsorbing to the paper, preventing the enzymes from amplifying nucleic acids. Enzymes are probably still adsorbing to the paper in our devices, but substrate turnover is not compromised, likely because these enzymes are undergoing straightforward hydrolysis reactions compared to amplifying nucleic acids. While the overall average V_{max} obtained by the program were similar between Whatman paper and transparency film, the errors obtained on transparency film were smaller compared to paper. Therefore, although enzyme activity is not compromised on PADs, plastic-based devices could provide more consistent results than paper-based devices. K_M increased and decreased for β-lactamase and β-glucuronidase, respectively, but the errors associated with the values were large enough to consider these results not statistically significant.

Conclusions and Future Directions

A new and accurate single-board computer program has been developed for automatically calculating enzyme kinetics on different device substrates based on color change. The developed program has been demonstrated in obtaining accurate values compared to manual analysis with a new code that averages most of the colored pixels present in a single sample spot using flood-fill. A new 3D-printed Raspberry Pi holder with an independent light source has also been developed for obtaining images for analysis that holds the Raspberry Pi board, camera, and devices for increased portability and user-friendliness. Although the box has been optimized for paper-based devices, our light diffusers will need to be further optimized for transparency-based devices to prevent reflections in the devices. Data obtained using the program so far has suggested that whether the device is fabricated with Whatman paper or transparency film, the apparent enzyme activity is not compromised. This hypothesis could be

further explored by calculating enzyme kinetics on various papers and polymers used in portable sensors.

While we demonstrated this system in obtaining Michaelis-Menten enzyme kinetic constants, the program could be modified for other colorimetric device applications. Because the program does not analyze a set number of pixels, but continues to analyze pixels until the device edge, it is not limited by device shape. The program currently obtains an average color intensity, then calculates the product formed over three minutes to calculate V_{max} and K_M of a specific enzyme. The program could be modified to relate the average color intensity back to a specific calibration curve and output an analyte concentration to the user, whether metals, pathogens, or biomarkers. Additionally, the program is currently measuring color intensity, but the program could be modified to count specifically colored pixels within a color intensity, enabling objective distance-based measurements. In future work, we plan to increase portability of the Raspberry Pi system by using a touch-screen interface instead of computer screen with connected keyboard and mouse, which is currently being used. User compatibility can also be improved by implementing graphic user interfaces (GUIs) for the user to simply click one button to run a program instead of running a program through a command center. With minor revisions to the code and these future implementations, this technology could be applicable for a large variety of colorimetric detection applications to eliminate the subjectivity currently seen in colorimetric paper-based devices.

Acknowledgements
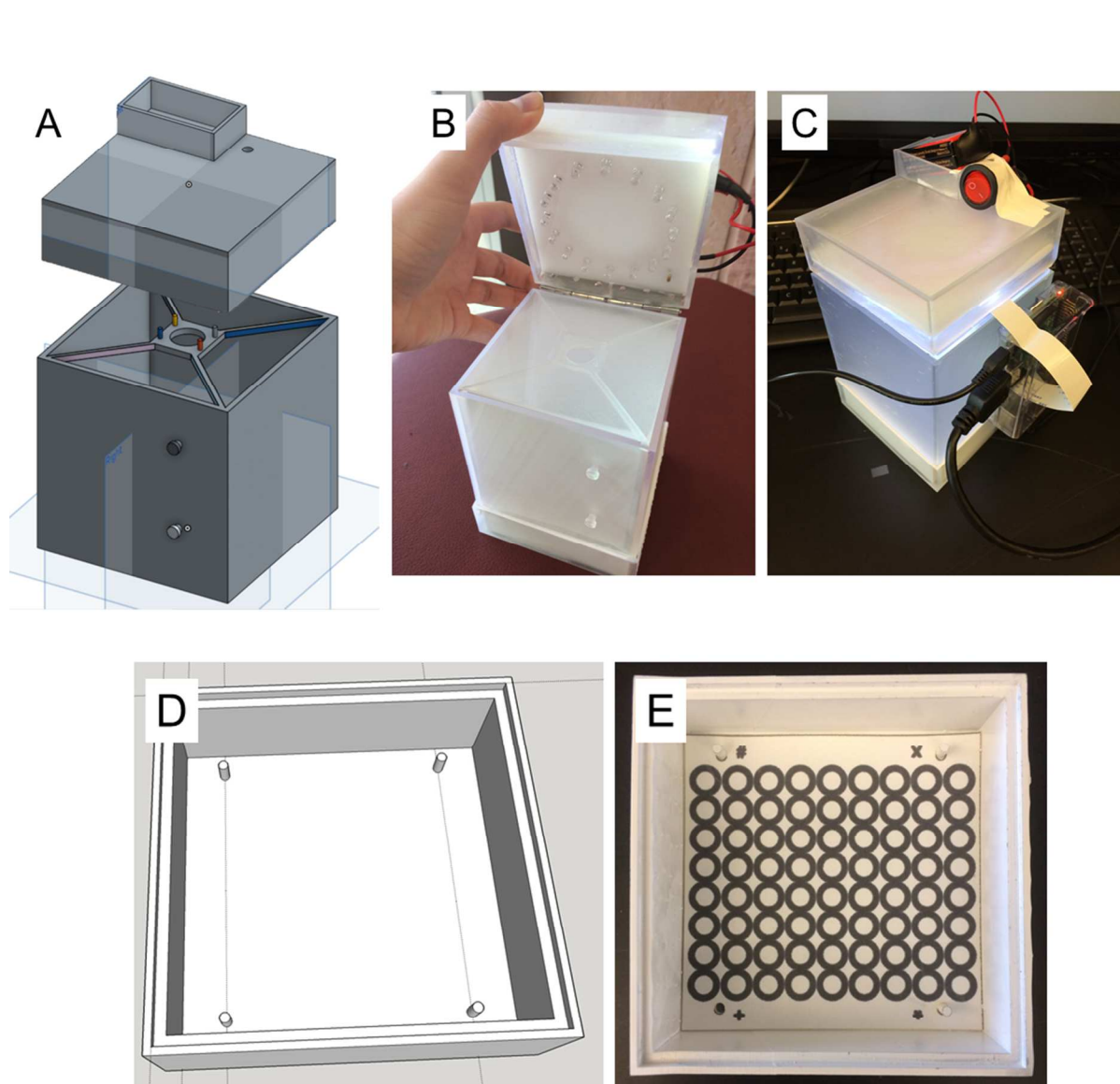
Figure 1 | The Raspberry Pi holder composed of two components to hold the Raspberry Pi board and camera (A-C) and paper- or transparency-based devices (D and E). **(A)** CAD image of Raspberry Pi holder and lid. **(B)** Lifting the lid of the final 3D-printed holder with lighting system enclosed in the lid. **(C)** Final system with Raspberry Pi held in place on the side of the holder. **(D)** CAD image of bottom component of holder that holds devices. **(E)** 3D-printed holder housing a paper-based device using pegs for consistent device placement.
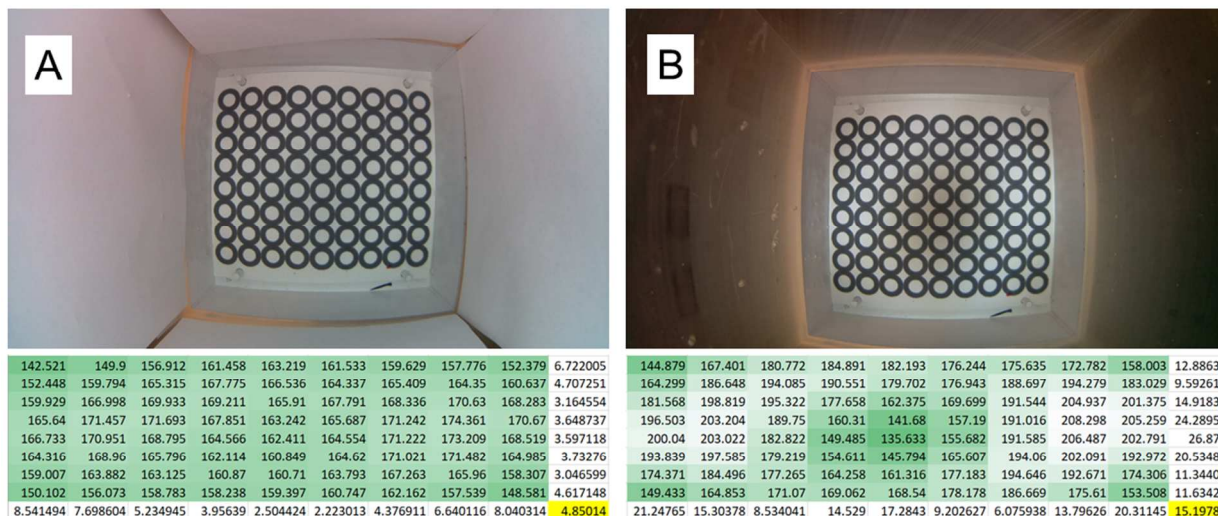
Figure 2 | Comparison of the best and worst distributions of light. **(A)** The best distribution of light was to line the holder with copy paper, have the plastic light diffuser with frosted side facing the paper-based device, and without a dark cover over the entire holder. **(B)** The worst distribution of light was no frosted plastic diffuser, no copy paper lining the sides, and with a dark cover over the entire holder.
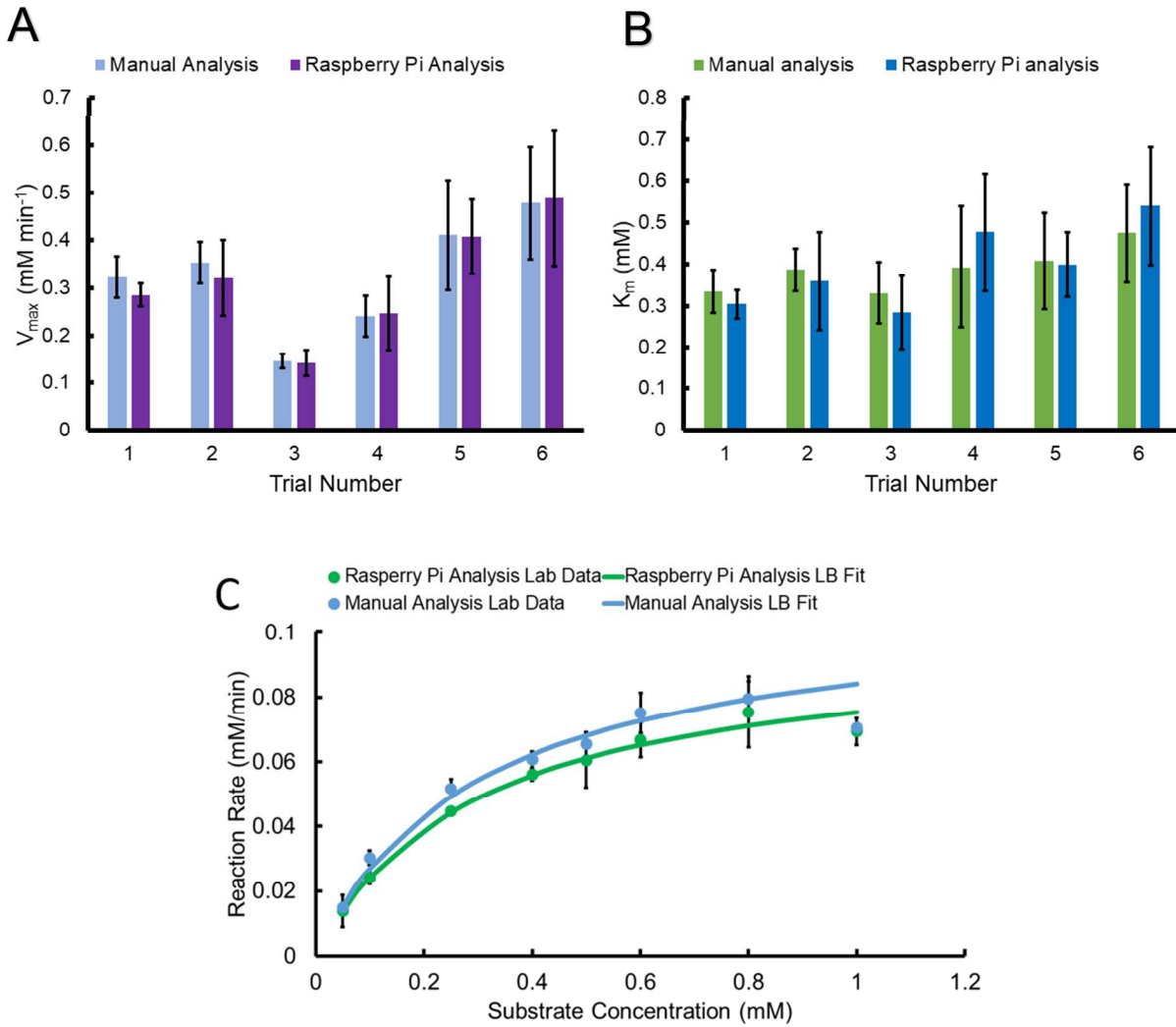
Figure 3 | Comparison of **(A)** V_{max} and **(B)** K_M through manual and Raspberry Pi image analysis using the final Raspberry Pi system. **(C)** An example Michaelis-Menten kinetics curve, comparing manual analysis to Raspberry Pi (RP) analysis. LB stands for Lineweaver-Burk fit, which is described in the materials and methods.
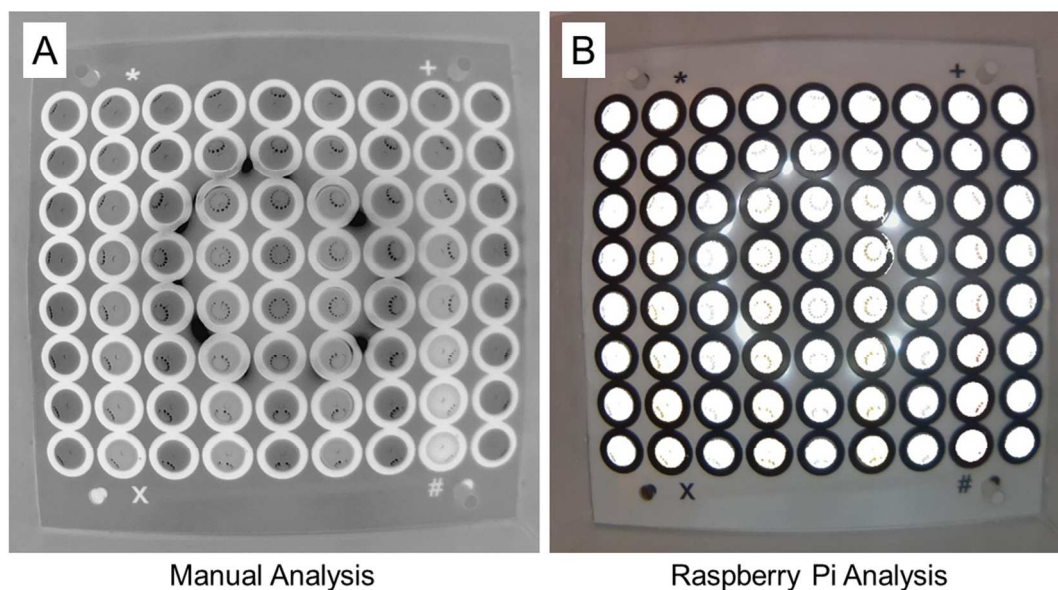
Figure 4 | Analyzing kinetic data on transparency sheets. **(A)** Kinetic experiment image that has been inverted to demonstrate that light ring reflection can affect data analysis. **(B)** Raspberry pi program using flood-fill algorithm to avoid these light reflections.
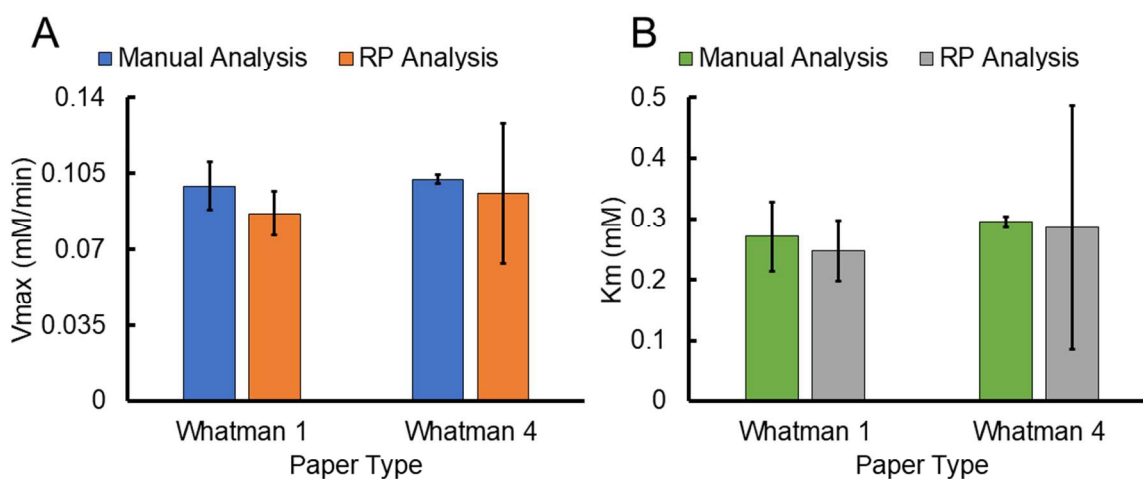
Figure 5 | Comparing kinetic data on different device platforms using two different enzymes. **(A)** V_{max} and **(B)** K_m of enzymes on paper- devices and transparency-based devices.

1
2
3
4
5
6
7
8
9
10
11
12
13
14
15
16
17
18
19
20
21
22
23
24
25
26
27
28
29
30
31
32
33
34
35
36
37
38
39
40
41
42
43
44
45
46
47
48
49
50
51
52
53
54
55
56
57
58
59
60

References

1. B. Srinivasan and S. Tung, *Journal of laboratory automation*, 2015, **20**, 365-389.
2. N. A. Meredith, C. Quinn, D. M. Cate, T. H. Reilly, 3rd, J. Volckens and C. S. Henry, *Analyst*, 2016, **141**, 1874-1887.
3. J. C. Jokerst, J. A. Adkins, B. Bisha, M. M. Mentele, L. D. Goodridge and C. S. Henry, *Anal Chem*, 2012, **84**, 2900-2907.
4. Y. Yang, E. Noviana, M. P. Nguyen, B. J. Geiss, D. S. Dandy and C. S. Henry, *Analytical Chemistry*, 2017, **89**, 71-91.
5. K. Yamada, H. Shibata, K. Suzuki and D. Citterio, *Lab on a Chip*, 2017, **17**, 1206-1249.
6. A. W. Martinez, S. T. Phillips, M. J. Butte and G. M. Whitesides, *Angew Chem Int Ed Engl*, 2007, **46**, 1318-1320.
7. M. M. Mentele, J. Cunningham, K. Koehler, J. Volckens and C. S. Henry, *Analytical chemistry*, 2012, **84**, 4474-4480.
8. H. I. Gomes and M. G. F. Sales, *Biosensors and Bioelectronics*, 2015, **65**, 54-61.
9. J. A. Adkins, K. Boehle, C. Friend, B. Chamberlain, B. Bisha and C. S. Henry, *Analytical Chemistry*, 2017, **89**, 3613-3621.
10. M. Srisa-Art, K. E. Boehle, B. J. Geiss and C. S. Henry, *Analytical Chemistry*, 2018, **90**, 1035-1043.
11. N. M. Rodriguez, J. C. Linnes, A. Fan, C. K. Ellenson, N. R. Pollock and C. M. Klapperich, *Analytical chemistry*, 2015, **87**, 7872-7879.
12. P. Teengam, W. Siangproh, A. Tuantranont, C. S. Henry, T. Vilaivan and O. Chailapakul, *Analytica Chimica Acta*, 2017, **952**, 32-40.
13. K. E. Boehle, J. Gilliand, C. R. Wheeldon, A. Holder, J. A. Adkins, B. J. Geiss, E. P. Ryan and C. S. Henry, *Angewandte Chemie International Edition*, 2017, DOI: 10.1002/anie.201702776, n/a-n/a.
14. U. H. Yildiz, P. Alagappan and B. Liedberg, *Analytical chemistry*, 2012, **85**, 820-824.
15. K. Talalak, J. Noiphung, T. Songjaroen, O. Chailapakul and W. Laiwattanapaisal, *Talanta*, 2015, **144**, 915-921.
16. D. M. Cate, J. A. Adkins, J. Mettakoonpitak and C. S. Henry, *Anal Chem*, 2015, **87**, 19-41.
17. G. G. Morbioli, T. Mazzu-Nascimento, A. M. Stockton and E. Carrilho, *Anal Chim Acta*, 2017, **970**, 1-22.
18. D. M. Cate, W. Dungchai, J. C. Cunningham, J. Volckens and C. S. Henry, *Lab Chip*, 2013, **13**, 2397-2404.
19. A. W. Martinez, S. T. Phillips, E. Carrilho, S. W. Thomas, 3rd, H. Sindi and G. M. Whitesides, *Anal Chem*, 2008, **80**, 3699-3707.
20. C. Sicard, C. Glen, B. Aubie, D. Wallace, S. Jahanshahi-Anbuhi, K. Pennings, G. T. Daigger, R. Pelton, J. D. Brennan and C. D. Filipe, *Water research*, 2015, **70**, 360-369.
21. T. S. Park, W. Li, K. E. McCracken and J. Y. Yoon, *Lab Chip*, 2013, **13**, 4832-4840.
22. M. M. Gong and D. Sinton, *Chemical Reviews*, 2017, **117**, 8447-8480.
23. Average selling price of smartphones worldwide from 2012 to 2017 (in U.S. dollars), https://www.statista.com/statistics/510668/smartphone-average-selling-price-worldwide/, (accessed 04/09/2018).
24. D. D. Luxton, R. A. Kayl and M. C. Mishkind, *Telemedicine and e-Health*, 2012, **18**, 284-288.
25. A. Robinson and M. Cook, *Raspberry Pi Projects*, John Wiley & Sons, 2013.
26. S. Jain, A. Vaibhav and L. Goyal, 2014.
27. M. N. Chowdhury, M. S. Nooman and S. Sarker, *Int. J. Sci. Eng. Res*, 2013, **4**, 550-558.
28. S. Ferdoush and X. Li, *Procedia Computer Science*, 2014, **34**, 103-110.
29. K. Bougot-Robin, J. Paget, S. C. Atkins and J. B. Edel, *Journal of Chemical Education*, 2016, **93**, 1232-1240.

30. G. Senthilkumar, K. Gopalakrishnan and V. S. Kumar, *International Journal of Emerging Trends & Technology in Computer Science*, 2014, **3**, 213-215.
31. G. Luka, E. Nowak, J. Kawchuk, M. Hoorfar and H. Najjaran, *Royal Society open science*, 2017, **4**, 171025.
32. G. Sharma and K. Kumar, *International Journal of Image, Graphics and Signal Processing*, 2017, **9**, 10.
33. J. Yu, L. Ge, J. Huang, S. Wang and S. Ge, *Lab on a Chip*, 2011, **11**, 1286-1291.
34. S. Nantaphol, O. Chailapakul and W. Siangproh, *Analytica chimica acta*, 2015, **891**, 136-143.
35. S. Z. Hossain, R. E. Luckham, M. J. McFadden and J. D. Brennan, *Analytical chemistry*, 2009, **81**, 9055-9064.
36. R. Nosrati, M. M. Gong, M. C. San Gabriel, C. E. Pedraza, A. Zini and D. Sinton, *Clinical chemistry*, 2016, **62**, 458-465.
37. T.-H. Yen, K.-H. Chen, M.-Y. Hsu, S.-T. Fan, Y.-F. Huang, C.-L. Chang, Y.-P. Wang and C.-M. Cheng, *Talanta*, 2015, **145**, 66-72.
38. B. Kannan, S. Jahanshahi-Anbuhi, R. H. Pelton, Y. Li, C. D. M. Filipe and J. D. Brennan, *Analytical chemistry*, 2015, **87**, 9288-9293.
39. S. Z. Hossain, C. Ozimok, C. Sicard, S. D. Aguirre, M. M. Ali, Y. Li and J. D. Brennan, *Analytical and bioanalytical chemistry*, 2012, **403**, 1567-1576.
40. B. Bisha, J. A. Adkins, J. C. Jokerst, J. C. Chandler, A. Perez-Mendez, S. M. Coleman, A. O. Sbodio, T. V. Suslow, M. D. Danyluk, C. S. Henry and L. D. Goodridge, *J Vis Exp*, 2014, DOI: 10.3791/51414.
41. E. Evans, E. F. M. Gabriel, W. K. T. Coltro and C. D. Garcia, *Analyst*, 2014, **139**, 2127-2132.
42. J. Linnes, N. Rodriguez, L. Liu and C. Klapperich, *Biomedical microdevices*, 2016, **18**, 30.
43. F. S. Teles, *Analytica Chimica Acta*, 2011, **687**, 28-42.
44. J. C. Linnes, N. M. Rodriguez, L. Liu and C. M. Klapperich, *Biomed Microdevices*, 2016, **18**, 30.